

Oliveira, Rafael; Claudino, Rafael; Kalid, Ricardo; Fröhlich, Thomas;
Gusmão, L.; Lepikson, Herman

Estimate of the inertial torque in rotating shafts - a metrological approach to signal processing

Original published in: 3rd International Congress on Mechanical Metrology (CIMMEC 2014) / CIMMEC 2014 - [Bristol] : IOP Publishing. - (2015), art. 012019, 11 pp. ISBN 978-1-5108-1475-2 (Journal of physics. Conference Series ; 648)

Conference: International Congress on Mechanical Metrology (CIMMEC) ; 3 (Gramado) : 2014.10.14-16

Original published: 2015-10-15

ISSN: 1742-6596

DOI: [10.1088/1742-6596/648/1/012019](https://doi.org/10.1088/1742-6596/648/1/012019)

[Visited: 2024-02-01]



This work is licensed under a [Creative Commons Attribution 3.0 Unported license](https://creativecommons.org/licenses/by/3.0/). To view a copy of this license, visit <https://creativecommons.org/licenses/by/3.0/>

Estimate of the inertial torque in rotating shafts - a metrological approach to signal processing

R Oliveira^{1,2}, R Claudino¹, R Kalid¹, T Fröhlich³, L Gusmão¹, H Lepikson¹

¹Universidade Federal da Bahia (UFBA), Salvador - BA, Brasil

²Instituto Nacional de Metrologia, Qualidade e Tecnologia (INMETRO), Rio de Janeiro - RJ, Brasil

³Technische Universität Ilmenau (TU-Ilmenau), Ilmenau, Alemanha

E-mail: rsoliveira@inmetro.gov.br

Abstract. This article studies the setting of the method to model the inertial torque in the acceleration regimes of a rotating axis system. The angular speed measurement to obtain an estimated acceleration and the moment of inertia axis of the variables are used to calculate the inertial torque. The evaluated dynamic regimes are acceleration ramps between levels (intervals) of angular speed, which are implemented using variable speed drives that are coupled to AC motors. The article focuses on assessing the main parameters in signal processing, such as the derivation of the speed signal, application of digital filters and data-smoothing methods, and their effects on the main features of interest in the generated torque curves, such as the peak torque amplitude, ascending and downward slopes, stability and repeatability. A qualitative approach was performed to identify the measurement uncertainty contributions. Thus, the validation methodology of the processing methods and the proposed physical principle are feasible.

1. Introduction

In systems or machines that use rotating shafts, the torque and angular velocity magnitudes are fundamentally important to the operation and characterization of most processes [1, 2, 3]. Examples of these operations are the positioning of a load, calculation of the transmitted mechanical power and restrictions on the acceleration regimes of equipment because of the inertial torque.

The load torque contributions can be estimated based on the direct correlation of weights, bending moments and assembly's friction characteristics for the displacements of load pieces. Therefore, its estimation is inserted to the definitions of the application's parameters such as the speed of operation and maximum efforts.

In the acceleration regimes, the inertial torque is an undesired behavior for setting the shaft driving. Thus, the angular acceleration regimes are often overdimensioned and function more as a safety and functional restriction when the acceleration periods are set to last long.

However, if the inertial torque response is more accurately estimated, the shaft driving can reach better performance with faster accelerations in different speed steps.

The angular velocity measurement with encoders is the usual method to estimate the inertial torque in the shaft instead of the direct measurement using torque or load sensors.



There are two torques on the axis during acceleration: the so-called load torque, which is generated from the resistance from the load to the movement, and the inertial torque, which is generated from the angular acceleration of the shaft masses and those attached to it.

One method to estimate the inertial torque is to use the product of the angular acceleration and the moment of inertia of the shaft. Generally, the moments of inertia are estimated quantities, which can be obtained from technical specifications of the components that are attached to the shaft.

In turn, the angular acceleration is generally estimated based on the angular speed signal, which is measured from the shaft. When measuring time-varying mechanical quantities, a dynamic error is introduced, i.e., the ratio between the input and the response cannot maintain itself as in static measurements. To mitigate these errors, the measured signal is post-processed, and the system dynamics modeling can be introduced [4]. Thus, the choice of a method or parameter to process the signal is an important step because the same signal-processing process can obtain different answers for different portions of the curve, which will result in loss of information or conversely, an unnecessary computational burden.

This paper presents a comparative study of some measurement and data-processing methods for the speed and acceleration, which relate the results to the regions and points of interest in the estimated inertial torque curves.

The purpose of the article is not to set or select the best method but to quantitatively demonstrate the difference among the obtained results and present a methodology that can be reproduced to validate these proceedings when they are applied.

2. Methodology

The research methodology was based on the data acquisition and manipulation of speed and torque under certain dynamical regimes from driving a measurement shaft. The acceleration and torque profiles are similar to the load impulses, where the peaks are fast, and these quantities did not have large stabilization levels and rates of change. These characteristics determine the dynamic schemes. According to the theory, the relationship between torque and angular acceleration should follow the physical principle of Newton's second law for angular movements, as shown in equation 1.

$$\tau = \theta \cdot \dot{\omega} \therefore \theta = \frac{\tau}{\dot{\omega}} \quad (1)$$

The experiments were performed at the Engine Test Laboratory of the Research Centre for Electric Energy (CEPEL). The bench (figure 1) consists of an electric motor, a variable speed drive, a torque transducer and an integrated speed sensor (incremental encoder), which were coupled in balance.

To define the type of regime under study, it is important to demonstrate the real profile of the curves or ramps controlled by the drives. The control parameters of the drives are adjusted for a particular application, so the inertial generated torque in the regime is used to calculate the minimum acceleration time. The theoretical equation obtained from the operating manuals of this equipment relates the rated power and rated speed with the acceleration and total moment of inertia to be accelerated [5]. However, this acceleration is assumed to be constant throughout the period, which is not consistent with the acceleration curves that are calculated from the angular-velocity measurements.

To illustrate this point, figure 2 shows two speed curves to fit the acceleration time of 2 s, which is set in the drive; one curve represents the theory, where the acceleration is considered constant, and the other curve represents the measured profile.

It is observed that the theoretical speed step is linear, which indicates a constant acceleration, which will approximately correspond to the mean of the measured acceleration, as shown in figure 3. This result is important because differences among the acceleration curves results in an even larger difference among the estimated inertial torques, which can determine the extra load on the shaft.

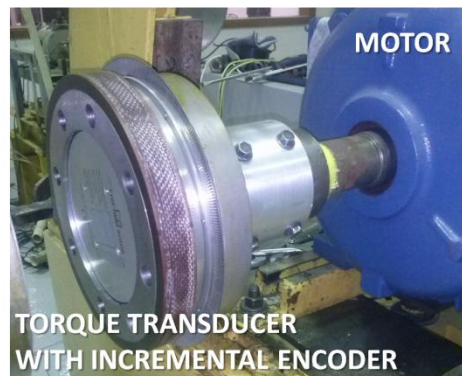


Figure 1. Test bench used in the experiment.

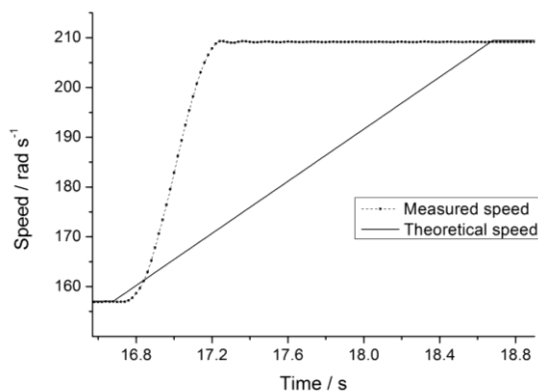


Figure 2. Acceleration ramp: measured speed and theoretical speed.

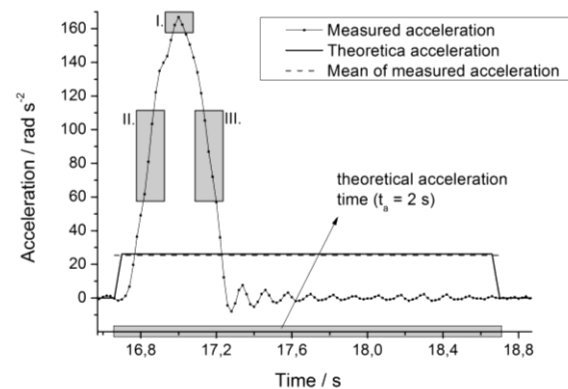


Figure 3. Acceleration curves: measured acceleration curve with identified critical regions and theoretical acceleration.

From the understanding of the applied real acceleration profile, the interesting regions of the curve can be determined to parameterize the inertial torque. In figure 3, these regions of interest were identified, considering the direct relationship between acceleration and torque: I) higher torque value (peak torque); II) higher positive torque rate; III) higher negative torque rate.

Then, the curves and methods were measured with the motor driving in steps of 52 rad s^{-1} in three different speed intervals: $157\text{-}209 \text{ rad s}^{-1}$, $209\text{-}261 \text{ rad s}^{-1}$ and $261\text{-}313 \text{ rad s}^{-1}$.

The acceleration time was set to 2 s, and the driving curves were repeated three times in each speed interval.

From the measured speed data, different commonly used signal-processing methods and tools were applied. The results were statistically analyzed using their nominal and dispersion values, considering the features and regions of interest in the driving curves, such as the peak accelerations and intermediate regions in the ascending and descending slopes of the curve.

The data treatment methods that were used are the commonly performed signal-processing methods with the identical characteristic regime, such as the components of moderate intensity noise and non-periodic instantaneous phenomenon to be measured. Some methods were applied to the original speed data (raw data), whereas others were applied to the calculated acceleration signal, which was obtained from the derivation of the original speed signal. A brief description of each applied method [6] is shown below.

Savitzky-Golay smoothing (SG) - The method performs a local polynomial regression around each point and creates a new smoothed value for each data point. This method preserves the data characteristics such as peak height and width. The softness depends on the window size (number of

points) to be used in the algorithm. For this analysis, windows with 15 points were used to smooth the original signals of the speed and the acceleration values. This method was also applied to smooth the torque signal.

Boltzman - This curve adjustment method produces a sigmoid response, which is notably similar to the driving results. It was only applied to the original speed signal.

Gauss - This method adjusts the data to a Gaussian curve, which is notably similar to the curves obtained for the acceleration profiles. It was only applied to the acceleration signals that are derived from the original speed signal.

Polynomial fit - Traditional method of polynomial regression. The software uses the least-square method. To make a comparison in the method, which is widely used in metrology, adjustments were made using a third-degree polynomial.

The measured torque values act as checker parameters of the adopted physical principle according to equation (1).

3. Results

The results are shown for each type of evaluation. Likewise, when appropriate, a brief conclusion or specific observations are shown. Subsections 3.1, 3.2, 3.3 and 3.5 are based on the same data that were measured on the three consecutive drives for each speed range at an acquisition rate of 50 Hz. For subsection 3.4, the acquisition rate varies as indicated.

3.1. Evaluation of the stability curves

This subsection shows the evaluation of the measurement stability during the acceleration in different speed ranges. The standard deviation was calculated from the speed and acceleration curves that were adjusted to the same time interval, i.e., the beginning of each acceleration ramp corresponds to time $t = 0$ s of the acceleration period. Figure 4 shows four speed deviations, whereas figure 5 shows the calculated acceleration deviation.

It is observed that the speed evaluation obtains smaller dispersions in the entire period of the curve than the acceleration evaluation. However, the center of the acceleration curve, where the peak is located, has higher stability, which is exactly the opposite of the observed behavior of speed curves.

It is also observed that the acceleration data that were calculated from the raw speed data have higher variation in standard deviation than those obtained from the smoothed data, filtered and fitted curves, which confirms the motivation for this study. Another important observation is that both curves were more stable in the range of 209-261 rad s^{-1} .

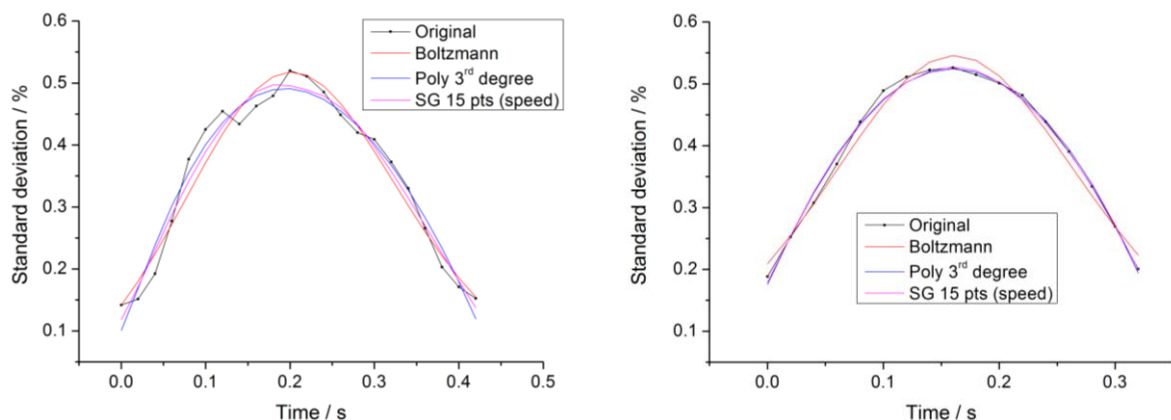


Figure 4. Standard deviation of each point of the speed curve among 3 sequential loadings in the speed intervals of (left) 157-209 rad s^{-1} and (right) 209-261 rad s^{-1} .

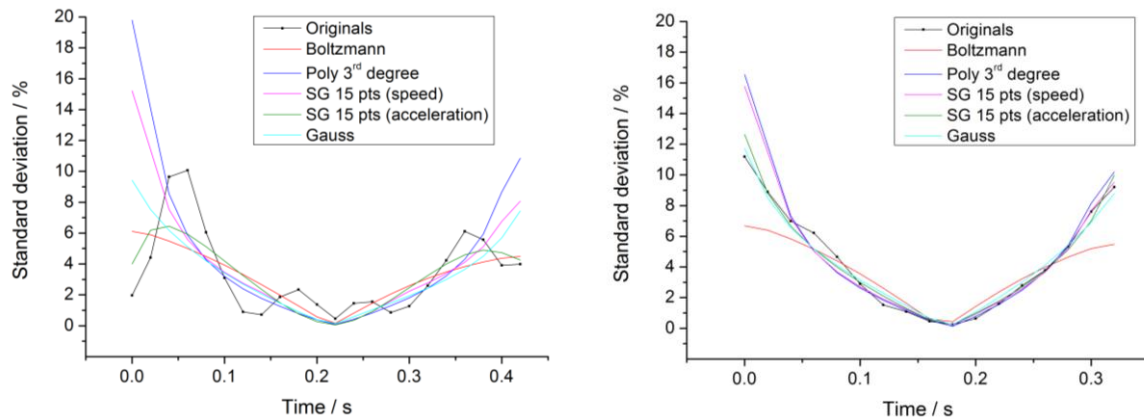


Figure 5. Standard deviation of each point of the acceleration curve among 3 sequential loadings in the speed intervals of (left) 157-209 rad s⁻¹ and (right) 209-261 rad s⁻¹.

3.2. Evaluation of peak acceleration

The peak acceleration corresponds to the peak torque and is the most critical region of the curve in terms of mechanical stress of the rotating shaft. Its variability was evaluated in different speed ranges under different acquisition rates and the results of different signal-processing methods that were applied to the same mass of data.

3.2.1. Peak variation among different speed ranges

Theoretically, at the identical degree of speed, which is 52 rad s⁻¹ in this case, the drive should apply the identical curve regardless of the acceleration speed range. However, table 1 shows a difference of the calculated peak values of different speed intervals.

Table 1. Nominal acceleration peaks of the three speed intervals.

	Speed interval / rad s ⁻¹		
	157 - 209	209 - 261	157 - 209
Acceleration peak/ rad s⁻²	166.39	202.62	241.36

3.2.2. Peak variation among different data-processing methods

In the same speed range, three consecutive measurements of acceleration ramps were performed. For the original mass of data, different signal-processing methods were implemented. Figure 6 shows the behavior that determines the peak in the first acceleration ramp of each method.

Table 2 shows the average peak in each method and the dispersion (standard deviation) among the three measurements. In this case, the results are shown for the intervals of 157-209 rad s⁻¹ and 209-261 rad s⁻¹.

In the first interval, the standard deviation of the processed data is better than that calculated from the original measurements. The second speed range curve has a lower derivation because the original measurements have better stability.

It is worth noting that in the first interval, the application of the SG smoothing method in both speed and acceleration signals produced identical results for the mean and standard deviation.

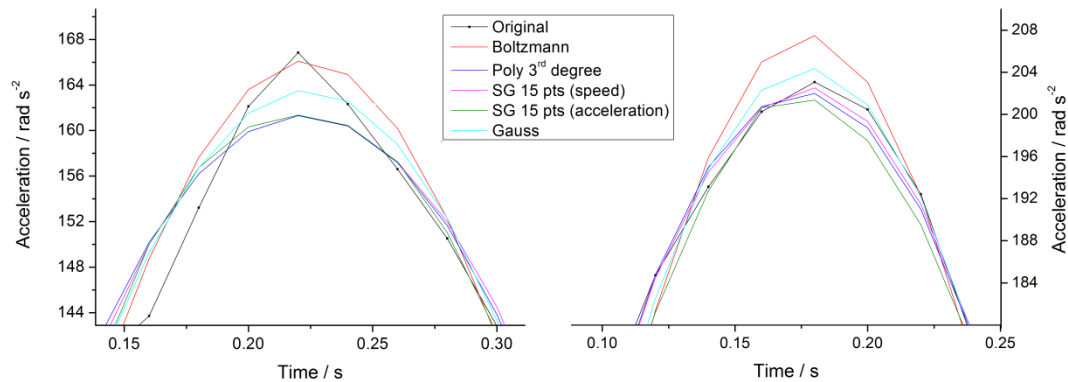


Figure 6. Acceleration peaks for different data-processing methods in the speed intervals of (left) 157-209 rad s^{-1} and (right) 209-261 rad s^{-1} .

Table 2. Mean and standard deviation of the acceleration peaks for the processing methods in different speed intervals.

Data processing method	Speed interval 157 - 209 rad s^{-1}		Speed interval 209 - 261 rad s^{-1}	
	Average peaks / rad s^{-2}	Standard deviation / %	Average peaks / rad s^{-2}	Standard deviation / %
Original	166.39	0.29	202.62	0.25
Boltzmann	166.14	0.16	207.17	0.16
Poly 3rd degree	161.42	0.080	202.00	0.13
SG 15 pts (speed)	161.29	0.052	202.34	0.078
SG 15 pts (acceleration)	161.29	0.052	201.56	0.33
Gauss	163.56	0.14	204.11	0.14

3.3. Evaluation of acceleration rates

The acceleration rates correspond to the variation of acceleration in time. This parameter is particularly important for applications that require torque as the control variable. Higher acceleration rates are more difficult to control, and better modeling can better model the control to predict these phenomena. The highest acceleration occurs on the ascending and descending sides of the acceleration ramps. The acceleration rates were calculated from the acceleration curves, and their maximum and minimum correspond to the peaks and valleys. Figure 7 shows the appearance of these curves for each data-processing method. The positive rate indicates an increasing acceleration (pre-peak), and the negative rate indicates a declining acceleration (post-peak).

To quantify these differences, table 3 shows the calculation of the standard deviation of peak rate with and without the methods that were used in two speed ranges.

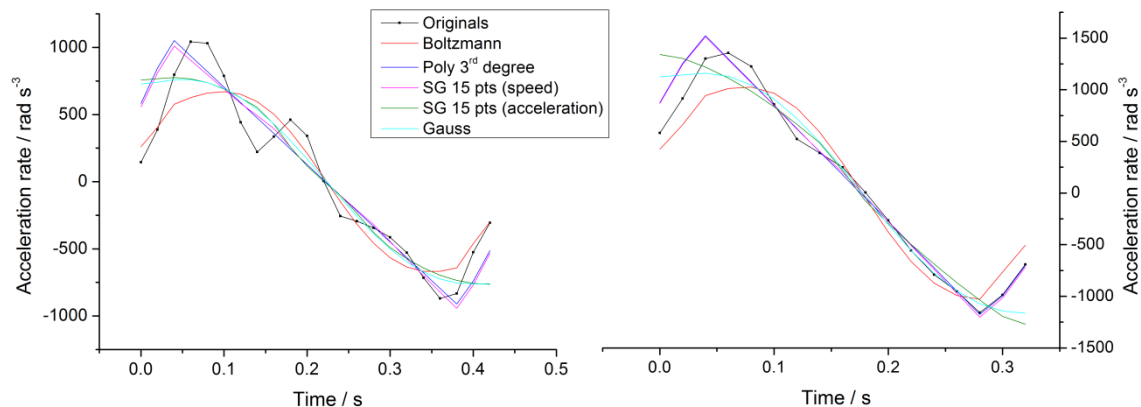


Figure 7. Acceleration rates for different data-processing methods in the speed intervals of (left) 157-209 rad s⁻¹ and (right) 209-261 rad s⁻¹.

Table 3. Mean and standard deviation of the peaks of acceleration rates for the processing methods in different speed intervals.

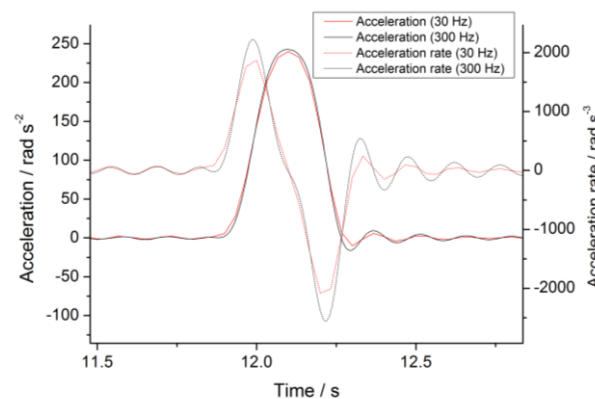
Data-processing method	Speed interval 157 - 209 rad s ⁻¹		Speed interval 209 - 261 rad s ⁻¹	
	Average peaks / rad s ⁻³	Standard deviation / %	Average peaks / rad s ⁻³	Standard deviation / %
Original	1123	7.4	1386	2.0
	-888	2.9	-1196	5.1
Boltzmann	672	0.88	1021	0.36
	-671	0.65	-1020	0.74
Poly 3rd degree	1042	3.2	1493	3.1
	-934	3.5	-1207	6.5
SG 15 pts (speed)	1018	1.6	1484	2.7
	-958	1.5	-1226	5.3
SG 15 pts (acceleration)	821	9.9	1375	2.2
	-773	9.8	-1306	3.4
Gauss	771	1.3	1176	1.3
	-772	1.2	-1177	1.0

3.4. Evaluation of different acquisition rates

A study was also conducted to evaluate the results of the same phenomenon measured at different acquisition rates. Table 4 shows the mean acceleration and deceleration rates and the standard deviation among the three ramps in each acquisition rate. Because of the operational limitations of the experiment, the experiment was only performed for the speed range of 261-313 rad s⁻¹. Figure 8 also illustrates different responses for acceleration and deceleration rates with the acquisition rates of 30 Hz and 300 Hz.

Table 4. Mean and standard deviation of the peaks of acceleration and acceleration rates for different acquisition rates in the speed interval of 261-313 rad s⁻¹.

Acquisition rates	Acceleration peaks		Peaks of positive acceleration rates		Peaks of negative acceleration rates	
	Mean/ rad s ⁻²	Standard deviation/ %	Mean/ rad s ⁻³	Standard deviation/ %	Mean/ rad s ⁻³	Standard deviation/ %
300 Hz	241.51	0.55	2244	0.93	-2567	1.5
100 Hz	244.68	1.26	2164	8.3	-2526	2.2
50 Hz	241.16	0.82	2115	5.2	-2409	3.9
30 Hz	239.95	0.35	1876	0.50	-2081	0.10

**Figure 8.** Acceleration curve and acceleration rate curve for different acquisition rates.

3.5. Data evaluation of torque

This study measured the torque to legitimize the principle of estimation of the inertial torque using the variables of equation (1). This inertial torque curve was estimated by multiplying the moment of inertia of the measurable portion of the transducer (θ_m) by the estimated acceleration in the speed ranges. According to the data sheet of the transducer, θ_m is approximately 0.00792 kg m² [7].

Figure 9 shows the torque curves that were obtained from the transducer-measured data and the estimated torque using θ_m and the speed data from the adjusted values, which were obtained using the SG method of 17 points.

Although there is a noticeable shift in both speed ranges, the curves have similar behaviors and no intersection. The changes during the peak acceleration because of the change in speed range also occur to the same extent for the variations of the peaks of the torque that was measured using the transducer.

Table 5 shows the results of peak torque and peak torque rate for each torque curve in different speed ranges. As with the acceleration rates, the torque rates were calculated based on the torque curves.

3.6. Measurement uncertainty

It is always important to evaluate the uncertainty of measurement for the proposed system or principle realization. Within the dynamic approach for metrology, in general, the traditional method of calculating the measurement uncertainty based on the ISO GUM [8] becomes incomplete when the magnitudes vary over time, the data are auto-correlated, and the assessment regimes are not stationary [9].

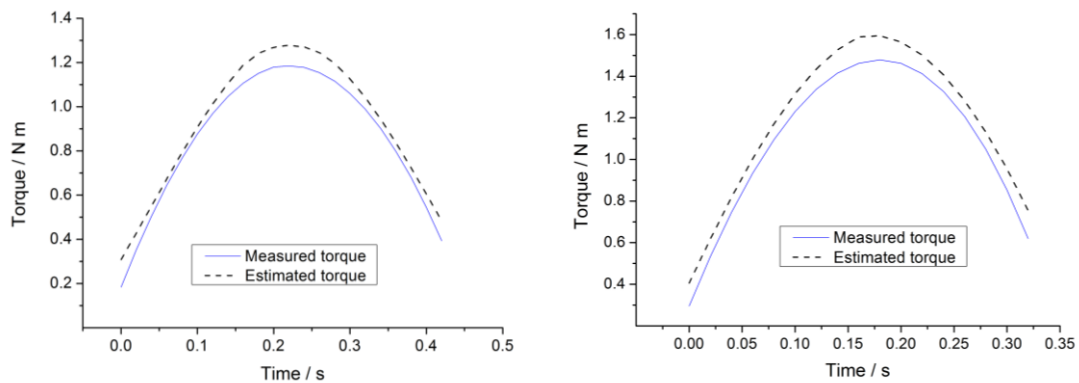


Figure 9. Measured torque and estimated torque curves in the speed intervals of (left) $157\text{-}209\text{ rad s}^{-1}$ and (right) $209\text{-}261\text{ rad s}^{-1}$.

Table 5. Mean and standard deviation of the acceleration peaks and acceleration rates for different acquisition rates in the speed interval of $261\text{-}313\text{ rad s}^{-1}$.

	Speed interval $157 - 209\text{ rad s}^{-1}$		Speed interval $209 - 261\text{ rad s}^{-1}$	
	Torque peaks/ N m	Torque rates/ N m s^{-1}	Torque peaks/ N m	Torque rates/ N m s^{-1}
Torque Measured	1.18	8.43 -7.53	1.48	11.83 -11.72
Torque Estimated	1.28	6.14 -6.06	1.59	10.62 -10.06

Then, a model is required to balance and consider these issues, which are particularities of dynamic processes, whether they are in the methodology of measurement, adjustment of the involved equipment or data-processing methods [10].

In the case of estimating the inertial torque, the evaluation of the data-processing method is one of the parameters that contribute to the measurement uncertainty. In the approach of modeling the inertial torque curves that are obtained when the shafts are accelerated by the motor drives, the contributions of measurement uncertainty follow the diagram in figure 10.

The dashed lines denote the uncertainty parameters in the validation of the data-processing method, where the repeatability of the parameters under various settings and the errors of indication or interpolation between the original acceleration signal and torque values were discussed in previous sections of this study.

Other contributions to the method validation such as the torque transducer uncertainty, encoder uncertainty and timer (clock) uncertainty of the acquisition system should be considered.

It is important to note that the method must be validated in a controlled environment with well known drives, where it is possible to simulate, evaluate and isolate the parameters of the curves to be studied or measure at the time of application and practical use of these devices, as shown in the previous sections.

However, in the usual applications of the inertial torque estimation, i.e., in the principal use of a shaft in an industrial process, other parameters should be considered and added to the uncertainty of the estimated torque, such as the encoder uncertainty, digital amplifier uncertainty, estimated moment

of inertia for the shaft and whenever possible, spot assessment of the repeatability and stability of the acceleration curves.

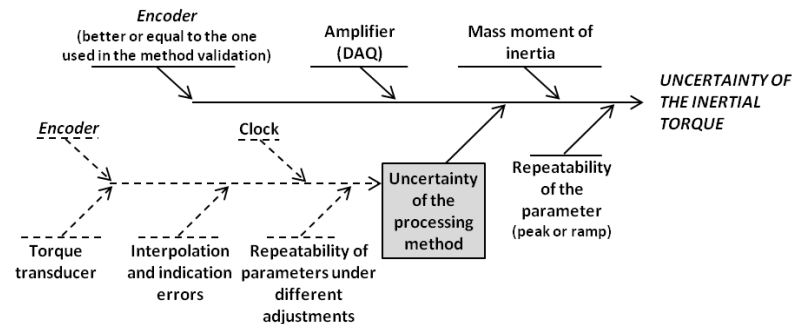


Figure 10. Diagram of the sources of measurement uncertainties in estimating the inertial torque.

4. Conclusion

Some issues were introduced regarding the necessity and applicability of the estimated inertial torque in driven rotating shafts. The physical principle adopted for this estimate using the acceleration and moment of inertia was presented and evaluated. In the acceleration curves that were obtained from the measurement practices, the regions of interest for the torque evaluation were defined, such as the slopes and peaks.

Because there are two dynamic regimes of measurement, the concept of dynamic error was introduced, and the study focused on evaluating some signal-processing methods of the involved acceleration and speed data, which should smooth these components.

These methods were compared using the repeatability and stability curves, where values were obtained to characterize the curve parameters, these measurement dispersions and the degree of consistency among the methods.

An introductory and qualitative approach was introduced to obtain the main contributions of measurement uncertainty of both the validation methodology of data processing and the inertial-torque estimation in its practical application.

Because this study aims to build a methodology to evaluate the equipment and concepts, it is concluded that although the results demonstrate the feasibility of applying the principles, the proposed foundations must be strengthened, and measurement practices were magnified by adding new equipment and quantification of other parameters involved, particularly those that were detected as uncertainty contributions, which were not addressed here. The torque transducer has a static calibration for its reference measured data, and this lack of dynamic traceability is also an object of parallel study by the authors.

Acknowledgments

The authors would like to thank the staff of the Motors Testing Laboratory of the Centro de Pesquisas em Energia Elétrica (CEPEL/Adrianopolis-RJ) for their support in performing the measurement practices, CNPq for the scholarships for scientific initiation and the Research Program Bragecrim (Capes/DFG) for the financial support and technical-cooperation viability.

References

- [1] Ovaska S J, Valiviita S 1998 Angular acceleration measurement: a review IEEE Transactions on Instrumentation and Measurement.
- [2] Gianfelici F 2005 A novel technique for indirect angular acceleration measurement CIMSA - IEEE International Conference on Computational Intelligence for Measurement Systems and Applications.

- [3] Capes/Bragecrim 2012 Research Project: DINTOR - Fundamentals for the Realization and Measurement of Dynamic Torque.
- [4] Website: <http://www.ptb.de/cms/en/fachabteilungen/abt8/fb-84/ag-842/dynamischemessungen-842.html> (jun/2014).
- [5] WEG "Motores Elétricos - Guia de Especificação".
- [6] Tutorial of the software OriginPro 8.5.0 SR1.
- [7] HBM Data-sheet of the transducer T10F.
- [8] BIPM, IEC, IFCC, ILAC, ISO, IUPAC, IU-PAP e OIML 2008 Evaluation of measurement data – Guide to the expression of uncertainty in measurement - GUM - JCGM 100.
- [9] Martins M A F, Kalid R 2010 Metodologia para avaliação da incerteza de medição em regime dinâmico de sistemas contínuos, COBEQ.
- [10] T Bruns, M Kobusch 2005 Data acquisition and processing for PTB's impact force standard machine IMEKO.